JACS
JOURNAL OF THE AMERICAN CHEMICAL SOCIETY
pubs.acs.org/JACS
Article

Enhancing the Equilibrium of Dynamic Thia-Michael Reactions through Heterocyclic Design

Alex E. Crolais,[§] Neil D. Dolinski,[§] Nicholas R. Boynton, Julia M. Radhakrishnan, Scott A. Snyder,* and Stuart J. Rowan*

Cite This: https://doi.org/10.1021/jacs.3c03643
Read Online
ACCESS | Metrics & More | Article Recommendations | Supporting Information

ABSTRACT: Although the catalyst-free dynamic thia-Michael (tM) reaction has been leveraged for a range of significant applications in materials science and pharmaceutical development, exploiting its full potential has been limited by relatively low equilibrium constants. To address this shortcoming, a new series of catalyst-free, room-temperature dynamic thia-Michael acceptors bearing an isoxazolone motif were developed and utilized to access both dynamic covalent networks and linear polymers. By leveraging the generation of aromaticity upon thiol addition and tuning the electronic-withdrawing/donating nature of the acceptor at two different sites, a wide range of equilibrium constants (K_{eq} ~1000 to ~100,000 M^{-1}) were obtained, constituting a 2 orders of magnitude increase compared to their noncyclic benzalcyanoacetate analogues. Integration into a ditopic isoxazolone-based Michael acceptor allowed access to both bulk dynamic networks and linear polymers; these materials not only exhibited tailorable thermomechanical properties based on thia-Michael acceptor composition, but the higher K_{eq} tM bonds resulted in more mechanically robust materials relative to past designs. Furthermore, solution-state formation of linear polymers was achieved thanks to the increased K_{eq} of the isoxazolone-based acceptors.

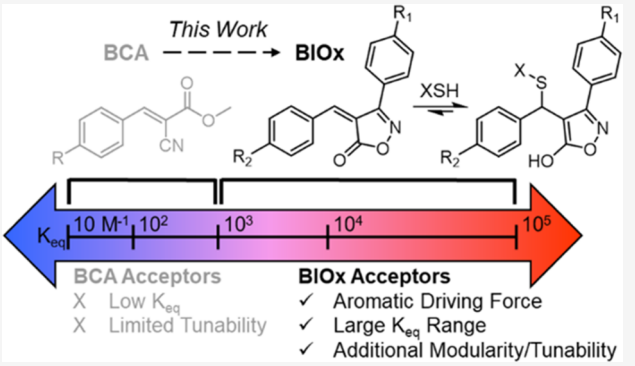

INTRODUCTION

The reversible and stimulus-responsive nature of dynamic covalent chemistries (DCC)[1,2] have long been exploited to access polymeric materials for applications ranging from drug delivery systems[3,4] and adhesives[5,6] to recyclable[7] and smart/adaptive materials.[8,9] Perhaps the most fundamental design parameter of such structurally dynamic polymeric materials is the choice of dynamic covalent bond incorporated into the system. Indeed, this feature determines the underlying properties of the material by modulating the exchange rate(s), equilibrium constant, catalyst requirements, and/or the identity of the external stimuli that may induce a response.[10,11] The variety of currently available dynamic bonds covers a wide swath of bonding partners, thereby facilitating a variety of synthetic installation approaches, with noteworthy examples including reversible Diels−Alder reactions,[12−16] alkyl urea exchange,[17,18] transesterification,[19,20] disulfide and diselenide exchange,[21−23] and many more.[24−28] However, as the scope of potential applications for DCC broadens, there remains a pressing need for the development of new, reversible covalent bonds. In particular, catalyst-free dynamic chemistries are attractive as they avoid the potential issues of catalyst-leaching and corresponding changes over time. Additionally, DCCs that operate under ambient conditions also have likely advantages in enabling enhanced exchange under typical operating conditions, although generally at the cost of the thermomechanical properties of the material (without reinforcement[29]), an issue which has presumably limited their study in materials applications to date.[30]

Thia-Michael (tM) chemistry, the conjugate addition of a thiol to an activated alkene under basic conditions, has been employed extensively in the synthesis and (post)-functionalization of polymers.[31] More recently, tM reactions have been explored as versatile, tunable dynamic bonding motifs. Notable examples include the use of thiol-acrylate[32] and thiol-maleimide[33] crosslinkers in self-healing materials. However, such dynamic tM materials require the presence of a base or elevated temperatures (90 °C) for exchange to occur. One interesting aspect of the tM reaction is its dynamic behavior can be tailored by the substituents on the activated alkene (Figure 1a), which has led to the continued exploration of tM bonds in dynamic networks.[34−36] In particular, the

Received: April 7, 2023

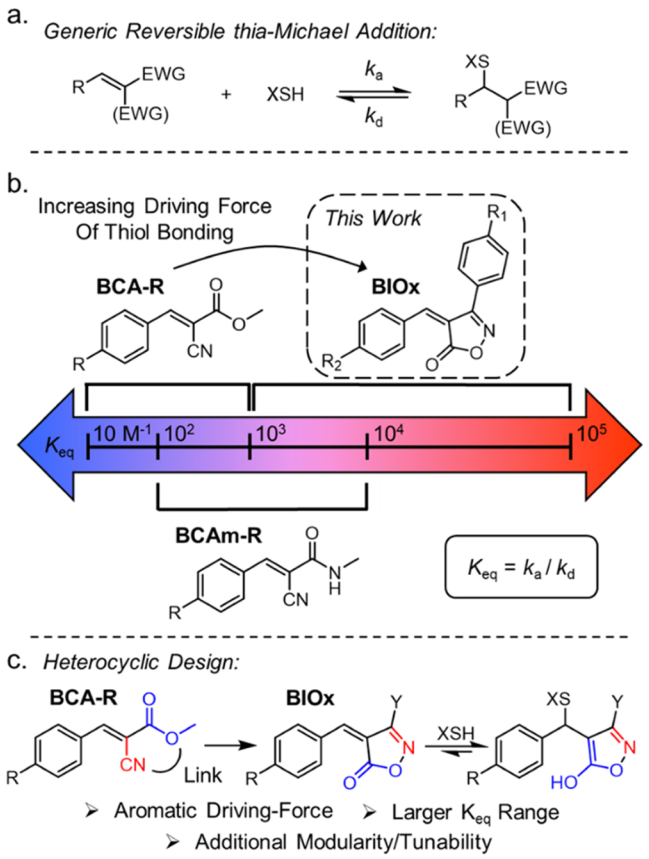

Figure 1. (a) General reaction scheme of dynamic thia-Michael reactions. Electron-withdrawing group in parentheses is not necessary for addition or reversibility. (b) Equilibrium constant (K_{eq}) ranges of the addition of thiols to benzalcyanoacetate (BCA), benzalcyanoacetamide (BCAm), and 3-substituted-4-benzalideneisoxazol-5(4H)one (BIOx) Michael acceptors. (c) Design of the proposed BIOx acceptors inspired by the BCA moiety in which the addition of a thiol yields aromatic 5-hydroxy isoxazole derivatives, which offer larger K_{eq} range and increased tunability.

benzalcyanoacetate (BCA) Michael acceptor, which has two electron-withdrawing groups, has allowed access to an interesting new class of dynamic systems.[37] Pioneering work into the BCA acceptor motif by the Taunton and Anslyn groups has demonstrated that in a polar solvent, these acceptors undergo thiol exchange at room temperature and in the absence of any catalyst.[38,39] Critically, varying the electron-donating/withdrawing properties of the β-phenyl ring has been shown to control the equilibrium constant, K_{eq}, of the thiol addition significantly (from ~10 to ~1000 M^{-1}).[39,40] These BCA acceptors have since been successfully incorporated into mechanically robust dynamic covalent network (DCN) films with shape memory behavior when prepared with tetra-functional thiols[40] or into multipurpose adhesives[41] upon mixing with poly(mercaptopropyl methyl)siloxane (PMMS). Importantly, the properties of such DCNs were shown to be readily tuned through the choice of substitution on the β-phenyl ring of the acceptor. However, despite their promising performance, their low K_{eq} range has limited the use of BCAs to solid-state networks, where the materials are reinforced by an emergent dynamic reaction-induced phase separation (DRIPS).[40]

While much of the focus in tunable tM dynamic bonds has revolved around manipulating the electronics of the β-phenyl ring, there are other handles to manipulate the K_{eq}. Any electron-withdrawing group (in the carbon acid precursor) directly attached to the double bond also has a significant effect on the thiol addition. For instance, it has been shown that replacing the ester in the BCA with an amide moiety results in a benzalcyanoacetamide (BCAm) Michael acceptor with enhanced thiol bonding, resulting in an ~10× enhancement in K_{eq} (~100 to ~10,000 M^{-1}) relative to BCAs.[39] The stronger bonding of BCAm acceptors has given access to a wider range of dynamic materials such as hydrogels,[42,43] stress-adaptive dense suspensions,[44] and other dynamic covalent networks.[45] Nevertheless, while these advances have already shown great promise in further manipulating the range of dynamic response in tM materials, the K_{eq} values are significantly lower than commonly employed supramolecular motifs used to access supramolecular polymers in solution (and in bulk).[46] Further increasing the K_{eq} range of dynamic tM acceptors (Figure 1b) would continue to expand their range of applications, particularly in allowing access to linear polymers with significant degrees of polymerization and potential uses in biological systems where efficacy at a low concentration is a requisite.[38]

Reported herein are studies aimed at developing catalyst-free, room-temperature dynamic thia-Michael bonds with significantly enhanced equilibrium constants (up to ~100,000 M^{-1}) along with initial explorations for their use in dynamic covalent polymers. Inspiration from the general structure of the BCA acceptor led to the exploration of new heterocyclic dynamic tM acceptors, where an isoxazolone (Figure 1c) is the cyclic analogue of methyl cyanoacetate (essentially linking the cyano and ester groups) and, as such, an imine now serves as the second withdrawing group instead of the cyano moiety. While such 3-substituted-4-benzylideneisoxazol-5(4H)-ones (BIOx) have been previously studied as dyes and for applications in α-propargylations, their efficacy as Michael acceptors, to the best of our knowledge, has never been investigated.[47,48] We hypothesized that the isoxazolone ring could offer two major advantages over its noncyclic analogue: (1) upon thiol addition to the BIOx acceptor, the resulting enol tautomer would yield an aromatic 5-hydroxy isoxazole moiety that could serve as a significant driving force for thiol addition and (2) a greater range of properties and equilibrium constants might be achieved given that these BIOx acceptors have an additional tuning handle through the "Y" position off of the imine linkage.

RESULTS AND DISCUSSION

As electronic substituents have been shown to have large effects on BCA tM acceptors, it was important to synthesize BIOx Michael acceptors with both the benzal moiety and a similarly substituted phenyl ring at the 3-position of the heterocycle (defined earlier as the "Y" position). The synthesis of the small-molecule BIOx acceptors could be accomplished in just two steps: (1) a ring closure between an appropriate aryl ketoester and hydroxylamine to yield the 3-substituted isoxazol-5(4H)-one and (2) a subsequent reaction with a substituted benzaldehyde via Knoevenagel condensation (Figure 2a). These materials were formed predominantly as the Z-isomer and could be synthesized in high yield (up to 90%).[48] In total, a series of 12 of these small-molecule BIOx acceptors ($\mathbf{1}_{R1,R2}$) were prepared, where R_1 and R_2 are the *para*-substituents on the aromatic groups at the 3- and 4-positions of the isoxazol-5(4H)-one, respectively.

https://doi.org/10.1021/jacs.3c03643
J. Am. Chem. Soc. XXXX, XXX, XXX−XXX

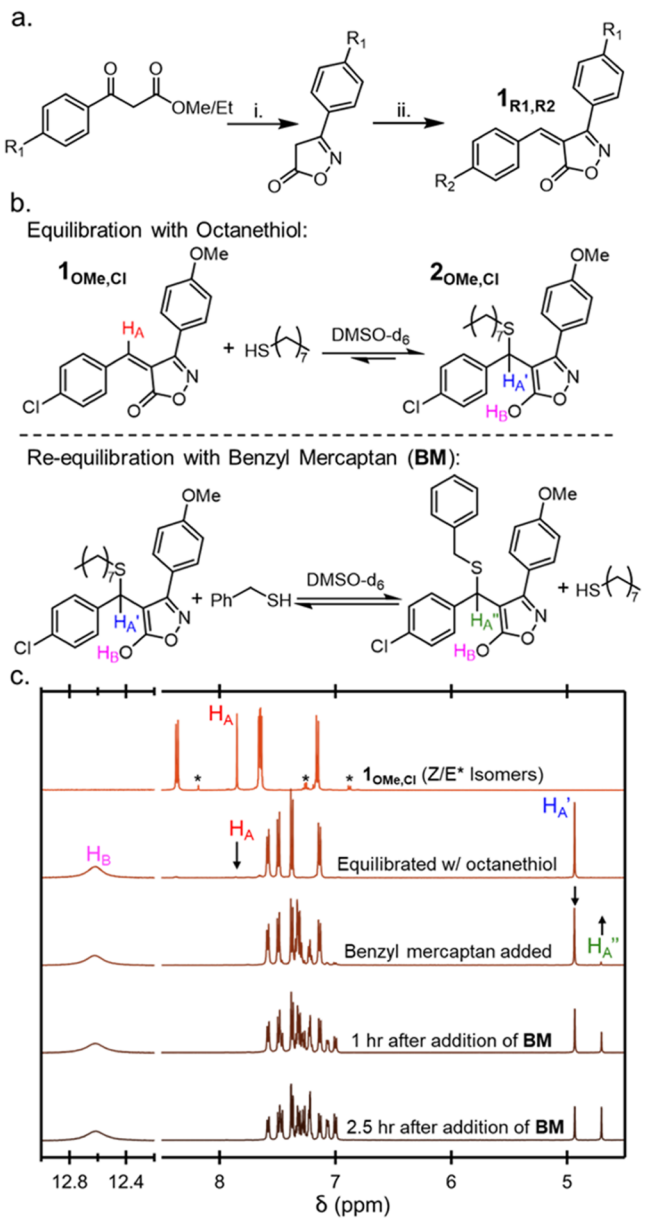

Figure 2. (a) Synthesis of $\mathbf{1}_{R1,R2}$ acceptors: (i) ketoester, hydroxylamine hydrochloride, NaOAc, ethanol, 50 °C, 93−99%; (ii) isoxazolone, benzaldehyde, piperidine, isopropanol, 50 °C, 25−90%. (b) Addition of nucleophile and (c) ^{1}H NMR spectrum of $\mathbf{1}_{OMe,Cl}$ after equilibration with octanethiol and during second equilibration with benzyl mercaptan (BM). The broad peak at 12.6 ppm is magnified by 5× for clearer visualization.

Initial small-molecule studies were performed to explore the reaction of a thiol with the BIOx acceptor $\mathbf{1}_{OMe,Cl}$. First, a solution of $\mathbf{1}_{OMe,Cl}$ (25 mM) was allowed to equilibrate with one equivalent of 1-octanethiol in DMSO-d_6. Within minutes of the thiol addition, a clear colorimetric shift from yellow to colorless was observed. Under ^{1}H NMR monitoring, nearly complete conversion of the olefin peak, H_A, to $\mathbf{2}_{OMe,Cl}$, H_A' (Figure 2b) was readily identified. The emergence of a broad downfield peak, H_B, at ∼12.5 ppm (along with the observation that H_A' is a lone singlet) confirmed the hypothesis that the aromatic enol product was formed upon thiol addition. These initial results demonstrated that BIOx acceptors allow the catalyst-free addition of a thiol in DMSO; however, it did not demonstrate that these tM adducts are dynamic at room temperature. To explore this element, one equivalent of benzyl mercaptan was then added to the equilibrated 1-octanethiol adduct solution and the resulting reaction was monitored *via* NMR. As shown in Figure 2b, shortly after the addition of the second thiol, a new peak, H_A'', began to appear as peak H_A' diminished, indicating thiol exchange was occurring in solution at room temperature. After 2.5 h, the two peaks reached equal intensity and reached equilibrium, confirming that these BIOx tM adducts are indeed dynamic at room temperature.

A signature feature of BCA acceptors is the ability to tune their K_{eq} through electronic modifications, as such an understanding of the impact of electronic modifications at the R_1 and R_2 positions is of interest for BIOx acceptors. To this end, the suite of $\mathbf{1}_{R1,R2}$ acceptors, whose R_1 and R_2 substituents range from electron-donating (-OMe; σ_{para} = -0.27) to electron-withdrawing (-Cl; σ_{para} = 0.23), had their equilibrium constants determined.[49] In order to accurately determine the equilibrium constants of $\mathbf{1}_{R1,R2}$, competition bonding experiments were performed on all acceptors (Figure 3a,b, see the SI for full details of the experimental setup and data interpretation, Figures S1 and S2). Excitingly, the isoxazolone-based tM acceptors displayed a range of K_{eq} values significantly higher (∼100×) than any previous BCA acceptor, with the highest K_{eq} (ca. 9.2 ± 0.3 × 10^4 M^{-1}) being observed for the thiol addition to $\mathbf{1}_{OMe,Cl}$. Furthermore, consistent with previously measured dynamic Michael acceptors,[39] the Hammett plot of the K_{eq} of the BIOx acceptors (Figure 3c) shows a positive trend (with a notable bend) with regard to the R_2 range from 1,100 M^{-1} ($\mathbf{1}_{H,OMe}$) to 80,000 M^{-1} ($\mathbf{1}_{H,Cl}$); this result highlights the impact of the electronic nature of the *β*-phenyl ring on the equilibrium. It is worthy of note that plotting K_{eq} against σ^+ Hammett parameters (Figure 3c inset) linearizes the plot, indicating a buildup of positive charge on the *β*-position in the transition state of the thia-Michael reaction. The importance of charge in the transition state can also be seen through changing solvent (polarity), with a significant slowdown in exchange measured when equilibration is carried out in $CDCl_3$ (Figure S4). Interestingly, the electronic nature of the R_1 substituent also had an effect on the thiol addition, albeit not as significant on account of R_1 being further removed from the *β*-position, leading to an ∼25% reduction in K_{eq} from $\mathbf{1}_{OMe,H}$ to $\mathbf{1}_{Cl,H}$. While there does appear to be a degree of interactivity between R_1 and R_2 positions, resulting in a shift from positive to negative correlations of R_1 with increasing R_2 withdrawing character, changes in K_{eq} through manipulating R_1 never exceeded ±2×. This finding implies that a combination of an electron-donating R_1 position and an electron-withdrawing R_2 position would lead to the highest K_{eq} values observed with $\mathbf{1}_{OMe,Cl}$.

With an understanding of how varied substituents impact the K_{eq} of the BIOx acceptors, a series of ditopic BIOx-bearing monomers were then prepared. As the R_2 position was shown to have the largest impact on the K_{eq} value, ditopic monomers linked to the BIOx moieties through the R_1 position were prepared. As the highest K_{eq}'s are observed with R_1 being an electron-donating group, ether bonds were chosen to attach the BIOx units. The synthesis of the requisite monomers was accomplished by generating two aryl ketoesters linked by triethylene glycol in the R_1 position; these compounds were then converted to the ditopic acceptor through a procedure similar to Figure 2a (see the SI for full scheme and synthetic details).[50−52] The synthesized ditopic BIOx monomers are

https://doi.org/10.1021/jacs.3c03643
J. Am. Chem. Soc. XXXX, XXX, XXX−XXX

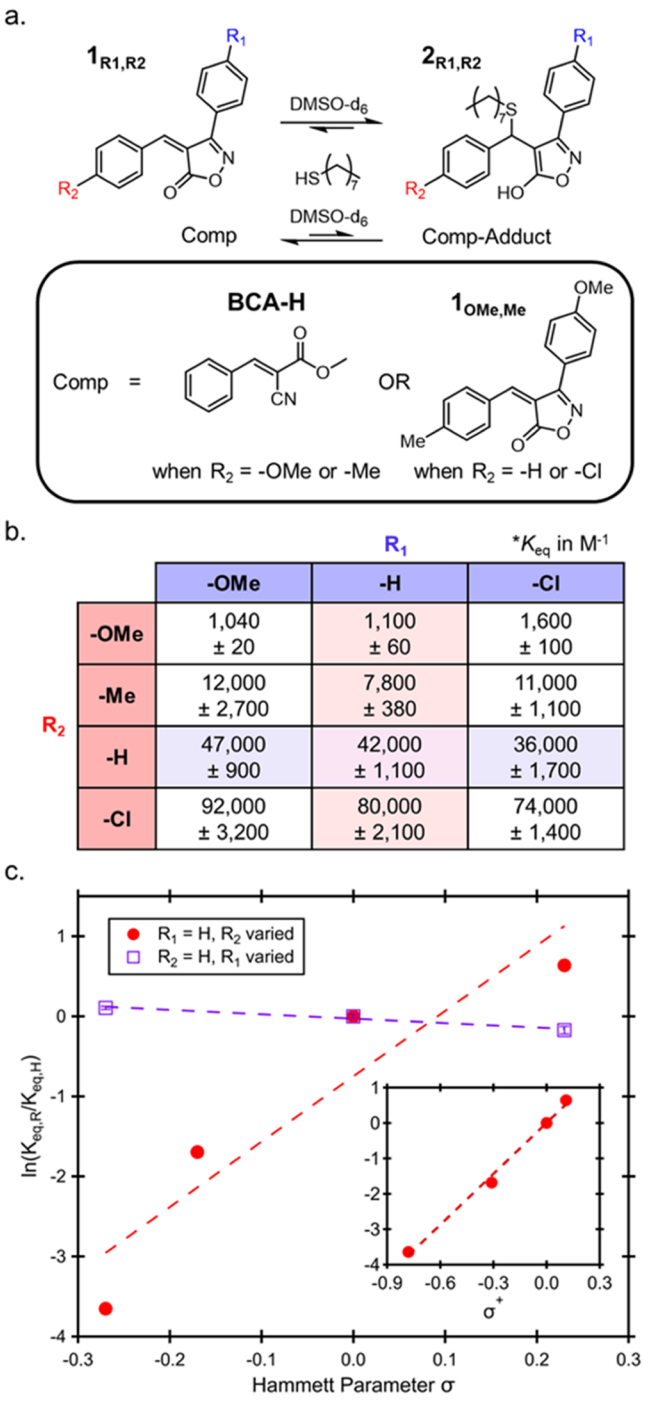

Figure 3. (a) Relevant equilibrium of competition K_{eq} study, (b) table of K_{eq} values of $\mathbf{1}_{R1,R2}$ tM acceptors, and (c) Hammett plot of $\mathbf{1}_{R1,H}$ (open square) and $\mathbf{1}_{H,R2}$ (red circle) sweeps (note that error bars are covered by the data points). The inset in (c) contains the $\mathbf{1}_{H,R2}$ sweep plotted using σ^+, linearizing the data.

referred to as $\mathbf{3}_R$, with R referring to the substituent at the R_2 position.

With a series of ditopic monomers $\mathbf{3}_R$ in hand, a set of dynamic covalent networks (DCN) were prepared with a tri-thiol crosslinker trimethylolpropane tris(3-mercaptopropionate) (TPTM). To prepare the networks, the desired $\mathbf{3}_R$ species was dissolved in $CHCl_3$ along with an equimolar (thiol/BIOx) amount of TPTM. The networks were then solution-cast and thoroughly dried to afford DCN films, $\mathbf{4}_R$ (Figure 4a). Complete removal of the $CHCl_3$ was confirmed through thermogravimetric analysis (TGA) (Figure S5). As a first assessment of the thermal properties of these $\mathbf{4}_R$ networks, differential scanning calorimetry (DSC) was performed (Figure 4b). In agreement with previously reported BCA-based networks,[40] both the $\mathbf{4}_{OMe}$ and $\mathbf{4}_{Me}$ curves display two

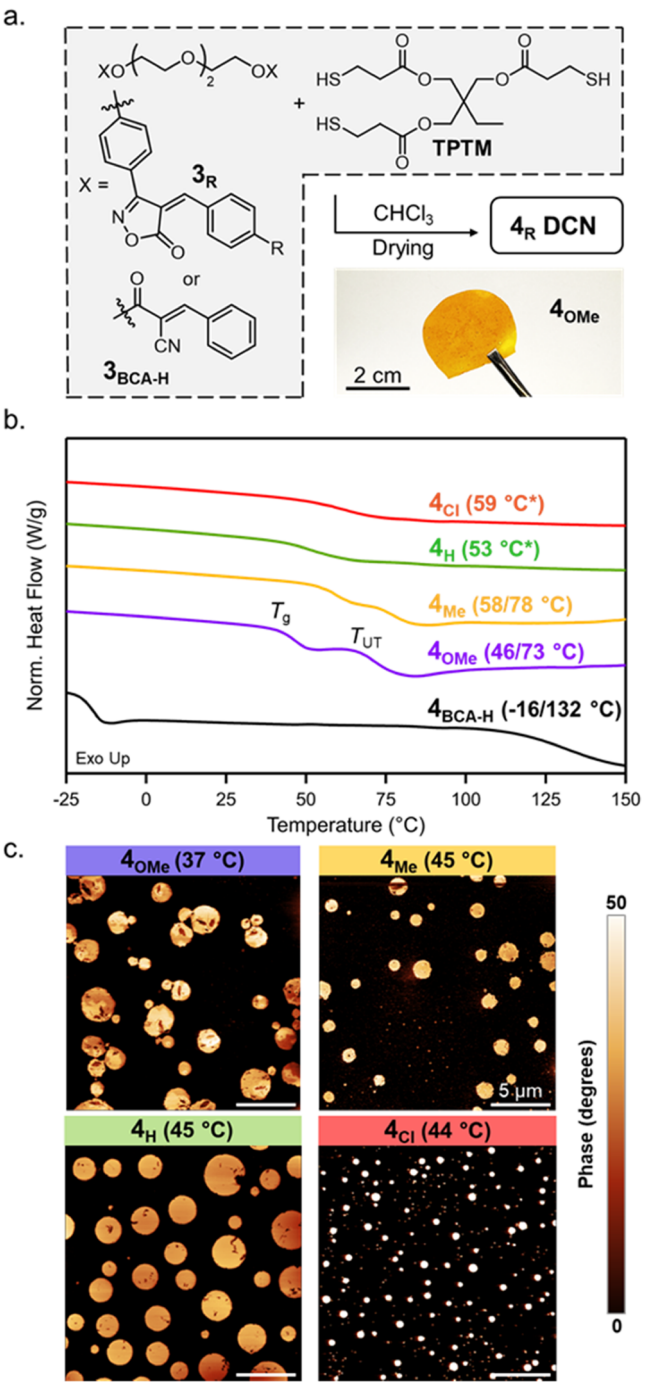

Figure 4. (a) Chemical structures used in the synthesis of bulk dynamic network and a representative photo of a $\mathbf{4}_{OMe}$ network after pressing. (b) Differential scanning calorimetry (DSC) curves for $\mathbf{4}_{Cl}$ (red), $\mathbf{4}_H$ (green), $\mathbf{4}_{Me}$ (orange), $\mathbf{4}_{OMe}$ (blue), and $\mathbf{4}_{BCA\text{-}H}$ (black). Values in parentheses represent the midpoints of T_g and T_{UT}, or the combined transition. (c) Atomic force microscopy (AFM) phase images of BIOx tri-thiol networks. Values in parentheses represent the temperature that the AFM was taken to maximize contrast.

https://doi.org/10.1021/jacs.3c03643
J. Am. Chem. Soc. XXXX, XXX, XXX−XXX

clear thermal transitions, consistent with the presence of multiple phases, and suggest that these two DCNs undergo a similar dynamic reaction-induced phase separation (DRIPS) process to the BCA networks.[40] The lower transition is attributed to the glass transition (T_g) of the continuous "soft" phase, while the higher transition is associated with the "hard" phase domains (T_{UT}). Interestingly, the higher K_{eq} materials ($\mathbf{4_H}$ and $\mathbf{4_{Cl}}$) displayed a singular broad transition, indicating that either there is no DRIPS process or that the T_g and T_{UT} have begun to converge. The convolution of T_g and T_{UT} was confirmed through modulated DSC of $\mathbf{4_H}$, which showed two transitions in the nonreversing heat flow curve (Figure S6). To further verify the phase-separated nature of these materials, atomic force microscopy (AFM) was carried out near T_g for each $\mathbf{4_R}$ network (Figure 4c), and in all cases, a phase-separated morphology was found. Similar to previous examples of DRIPS,[40] the underlying equilibrium constants do not obviously correlate with the observed morphologies, indicating that additional factors (such as sterics, solubility, etc.) strongly contribute to the DRIPS process. While DRIPS is key to the robust properties of BCA-based networks, it was hypothesized that the enhanced equilibrium of BIOx-based networks would give access to thermomechanically robust materials properties above their relatively low T_{UT}.

To further probe the effects of the equilibrium constant on the thermomechanical properties of the networks, small-amplitude oscillatory shear (SAOS) rheology studies were carried out (Figure 5a). In agreement with the trends in thiol affinity, the increased electron-withdrawing character of the key substituents was found to result in higher glass-transition temperatures (as defined by the peak in tanδ), ranging from ca. 65 to 85 °C from $\mathbf{4_{OMe}}$ to $\mathbf{4_{Cl}}$. The high T_g values of the $\mathbf{4_R}$ networks are in stark contrast to an analogous BCA-based network, whose T_g was found to only be ∼10 °C. Interestingly, the electron-rich crosslinkers ($\mathbf{4_{OMe}}$ and $\mathbf{4_{Me}}$), whose K_{eq} values are similar to the highest available BCA/BCAm acceptors, were found to freely flow shortly after rising above T_g, due to insufficient bonding to maintain percolation at elevated temperatures (Figure 5a). However, further increases in the K_{eq} were found to lead to more robust behavior at higher temperatures, with both $\mathbf{4_H}$ and $\mathbf{4_{Cl}}$ displaying rubbery plateaus, with $\mathbf{4_{Cl}}$ having the highest modulus (extent of crosslinking) and largest range spanning ca. 100−140 °C. Importantly, all networks were found to readily undergo reprocessing through melt pressing conditions, with limited to no changes in thermal transitions, optical clarity, or thermomechanical properties across reprocessing steps (Figures S8−S10). It is worthy of note that while these materials can be reprocessed, it was found that extended exposure to temperatures ∼150 °C induces irreversible crosslinking events (Figure S11).

Given the extended plateau behavior of $\mathbf{4_{Cl}}$, additional stress relaxation experiments were carried out (Figure 5b). At all measured temperatures, the material was shown to relax and the resulting data is well described by a stretched exponential fit (eq 1).

$$G_t/G_0 = e^{-(t/\tau^*)^{\alpha}} \quad (1)$$

This function is employed to describe a distribution of relaxation rates throughout the network and allowed for the determination of τ^* for networks that did not relax beyond $G_t/G_0 = e^{-1}$ (denoted by open symbols). The relaxation was

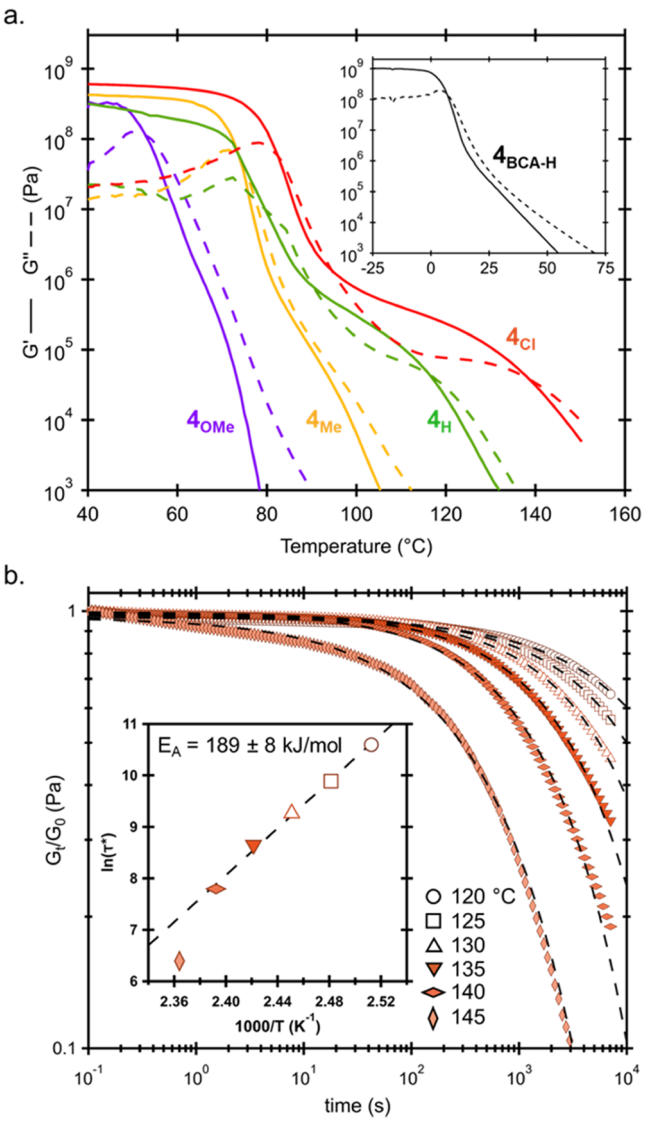

Figure 5. (a) Shear rheology (temperature ramp rate 3 °C/min, frequency = 1 Hz, parallel-plate geometry) for $\mathbf{4_{Cl}}$ (red), $\mathbf{4_H}$ (green), $\mathbf{4_{Me}}$ (orange), $\mathbf{4_{OMe}}$ (blue), and $\mathbf{4_{BCA\text{-}H}}$ (black) and (b) stress relaxation (3% strain) curves for $\mathbf{4_{Cl}}$ at 120 °C (open circle), 125 °C (open square), 130 °C (open triangle), 135 °C (orange triangle), 140 °C (horizontal diamond), and 145 °C (vertical diamond). Open plots indicate τ^* extrapolated from the curve.

found to be Arrhenius up to 140 °C, before deviating at higher temperatures, a feature observed before in dissociative networks.[53] Further analysis of the stress relaxation data indicates that the apparent viscosity of the network drops precipitously above 140 °C (Figure S14), consistent with a significant decrease in network connectivity. Impressively, the extracted activation energy from the Arrhenius portion was found to be 189 kJ/mol, indicating the relaxation process (related to k_d) is highly dependent on temperature.[54] To further examine this effect, creep experiments were performed on $\mathbf{4_{Cl}}$ at various temperatures (Figure S15). In agreement with the results from the stress relaxation experiment, the rate of creep was highly dependent on temperature, with an ∼250× increase in the steady-state rate of creep over a 20 °C range (0.01 to 2.55 s^{-1} for 90 and 110 °C, respectively).

While the ability to widely tune the bulk network properties through electronic modifications is an attractive feature of

https://doi.org/10.1021/jacs.3c03643
J. Am. Chem. Soc. XXXX, XXX, XXX−XXX

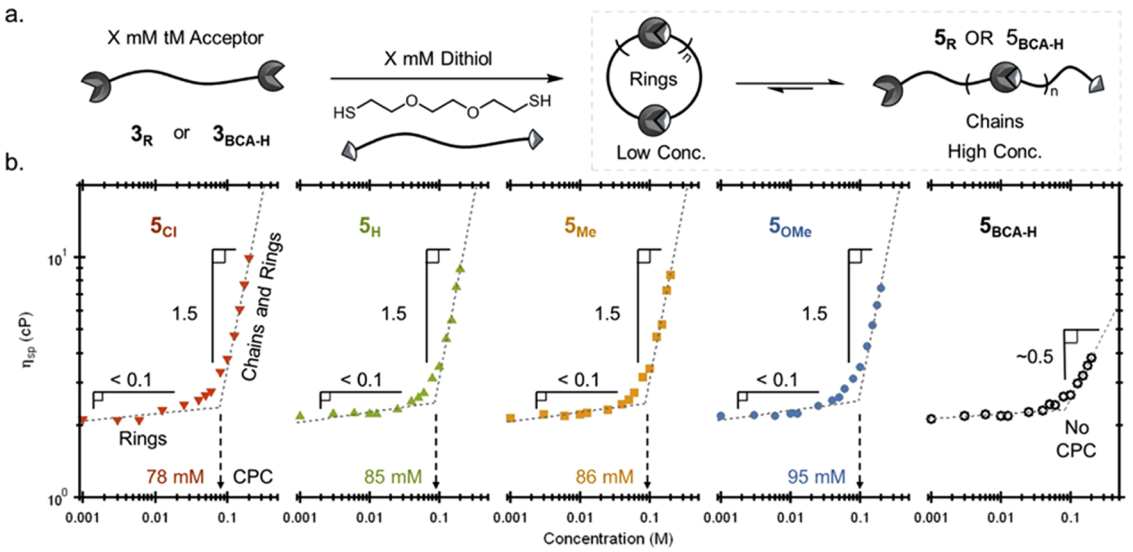

Figure 6. (a) Synthesis of $\mathbf{5}_{R}$ and $\mathbf{5}_{BCA\text{-}H}$ linear polymers and (b) log−log plots of zero shear viscosity versus concentration of $\mathbf{5}_{Cl}$ (red triangle), $\mathbf{5}_{H}$ (green triangle), $\mathbf{5}_{Me}$ (orange square), $\mathbf{5}_{OMe}$ (blue circle), and $\mathbf{5}_{BCA\text{-}H}$ (open circle).

BIOx acceptors, the high K_{eq} values of the synthesized acceptors are not a requirement. To highlight the utility of these enhanced tM acceptors, their use in solution polymerization with bis-thiol monomers, where molecular weight is strongly controlled by K_{eq}, was investigated. Thus, solutions of $\mathbf{3}_{R}$ and 2,2′-(ethylenedioxy)diethanethiol of varying concentrations ranging from 1 mM to 200 mM were prepared in dry DMSO and allowed to equilibrate overnight before solution viscometry measurements were carried out to follow the polymerization reaction (Figure 6a). The zero shear specific viscosities (η_{sp}) were extrapolated from shear rate sweeps (see representative viscosity vs shear rate plot for $\mathbf{5}_{H}$, Figure S16) and were plotted against the concentration to reveal different regimes of the polymerization (Figure 6b). Log−log plots of η_{sp} vs concentration provide structural insights into the solution polymers, allowing for the determination of the critical polymerization concentrations (CPC) for the ditopic acceptors, where linear polymer formation begins to dominate over the formation of oligomeric cyclic structures.[46,55] Here, the transition to a slope of ∼1.5 is indicative of the formation of linear chains, which all four BIOx crosslinkers were able to achieve. In agreement with the trend in their K_{eq} values, the CPCs of $\mathbf{5}_{Cl}$, $\mathbf{5}_{H}$, $\mathbf{5}_{Me}$, and $\mathbf{5}_{OMe}$ were found to be 78, 85, 86, and 95 mM (corresponding to extents of association of ∼99, 99, 98, and 93%), respectively. Additionally, it was also noted that $\mathbf{5}_{Cl}$ had the highest viscosity at 200 mM, with descending values moving to $\mathbf{5}_{OMe}$, implying higher overall degrees of polymerization. As expected, increasing the temperature was found to increase the CPC; in the case of $\mathbf{5}_{H}$ measured at 50 °C, the CPC was found to increase to 99 mM (Figure S17), corresponding to an expected extent of association of ∼96%.

To emphasize the importance of the enhanced K_{eq} values, this experiment was also performed using an analogous BCA crosslinker, which did not prove capable of forming linear polymers in the same concentration regime (max slope ∼0.5, Figure 6b).

CONCLUSIONS

In summary, a new class of isoxazolone-based tM acceptors have been readily synthesized and shown to be a versatile new class of room-temperature, tunable, and catalyst-free dynamic motifs. This heterocyclic electrophile design takes advantage of aromatization upon thiol addition, resulting in an enhanced K_{eq} range up to ∼10^5 M^{-1}. Electronic manipulation of both the R_1 and R_2 positions results in predictable equilibrium constant changes, with R_2 having a significantly stronger effect. Incorporating these acceptors into linear polymers and bulk networks allows for an impressive range of tunable mechanical properties that are accessible from a polymer containing room-temperature dynamic bonds. The high tunability of the tM acceptor combined with the ability to access high equilibrium constants offer a route to access mechanical robust stimuli-responsive materials that are adaptive at room temperature; such studies are the subject of current investigations and will be reported in due course.

ASSOCIATED CONTENT

Supporting Information

The Supporting Information is available free of charge at https://pubs.acs.org/doi/10.1021/jacs.3c03643.

Synthetic procedures, material characterization including NMR experiments, TGA, DSC, shear rheology, AFM, and viscometry measurements (PDF)

AUTHOR INFORMATION

Corresponding Authors

Scott A. Snyder − *Department of Chemistry, University of Chicago, Chicago, Illinois 60637, United States;* orcid.org/0000-0003-3594-8769; Email: sasnyder@uchicago.edu

Stuart J. Rowan − *Department of Chemistry and Pritzker School of Molecular Engineering, University of Chicago, Chicago, Illinois 60637, United States;* orcid.org/0000-0001-8176-0594; Email: stuartrowan@uchicago.edu

Authors

Alex E. Crolais − *Department of Chemistry, University of Chicago, Chicago, Illinois 60637, United States*

Neil D. Dolinski − *Pritzker School of Molecular Engineering, University of Chicago, Chicago, Illinois 60637, United States;* orcid.org/0000-0002-2160-8811

https://doi.org/10.1021/jacs.3c03643
J. Am. Chem. Soc. XXXX, XXX, XXX−XXX

Nicholas R. Boynton − *Pritzker School of Molecular Engineering, University of Chicago, Chicago, Illinois 60637, United States*

Julia M. Radhakrishnan − *Department of Chemistry, University of Chicago, Chicago, Illinois 60637, United States*

Complete contact information is available at: https://pubs.acs.org/10.1021/jacs.3c03643

Author Contributions

§A.E.C. and N.D.D. contributed equally. The manuscript was written through contributions of all authors. All authors have given approval to the final version of the manuscript.

Notes

The authors declare no competing financial interest.

■ ACKNOWLEDGMENTS

This work was supported by the Division of Materials Research of the NSF (award #2104694) and by the University of Chicago. NDD thanks the Pritzker School of Molecular Engineering for support through a postdoctoral fellowship. N.R.B. was supported by a NASA Space Technology Graduate Research Opportunities Award. Parts of this work were carried out at the Soft Matter Characterization Facility of the University of Chicago. This work made use of the shared facilities at the University of Chicago Materials Research Science and Engineering Center, supported by National Science Foundation under award number DMR-2011854. The authors also thank Dr. Josh Kurutz and Dr. C. Jin Qin for assistance with NMR and mass spectrometry, respectively.

■ REFERENCES

(1) Rowan, S. J.; Cantrill, S. J.; Cousins, G. R. L.; Sanders, J. K. M.; Stoddart, J. F. Dynamic Covalent Chemistry. *Angew. Chem.- Int. Ed.* **2002**, *41*, 898−952.

(2) Wojtecki, R. J.; Meador, M. A.; Rowan, S. J. Using the Dynamic Bond to Access Macroscopically Responsive Structurally Dynamic Polymers. *Nat. Mater.* **2011**, *10*, 14−27.

(3) Ulrich, S. Growing Prospects of Dynamic Covalent Chemistry in Delivery Applications. *Acc. Chem. Res.* **2019**, *52*, 510−519.

(4) Zhu, Q.; Saeed, M.; Song, R.; Sun, T.; Jiang, C.; Yu, H. Dynamic Covalent Chemistry-Regulated Stimuli-Activatable Drug Delivery Systems for Improved Cancer Therapy. *Chin. Chem. Lett.* **2020**, *31*, 1051−1059.

(5) Wang, Z.; Guo, L.; Xiao, H.; Cong, H.; Wang, S. A Reversible Underwater Glue Based on Photo- and Thermo-Responsive Dynamic Covalent Bonds. *Mater. Horiz.* **2020**, *7*, 282−288.

(6) Lamping, S.; Otremba, T.; Ravoo, B. J. Carbohydrate-Responsive Surface Adhesion Based on the Dynamic Covalent Chemistry of Phenylboronic Acid- and Catechol-Containing Polymer Brushes. *Angew. Chem., Int. Ed.* **2018**, *57*, 2474−2478.

(7) Ogden, W. A.; Guan, Z. Recyclable, Strong, and Highly Malleable Thermosets Based on Boroxine Networks. *J. Am. Chem. Soc.* **2018**, *140*, 6217−6220.

(8) Kloxin, C. J.; Bowman, C. N. Covalent Adaptable Networks: Smart, Reconfigurable and Responsive Network Systems. *Chem. Soc. Rev.* **2013**, *42*, 7161−7173.

(9) Kloxin, C. J.; Scott, T. F.; Adzima, B. J.; Bowman, C. N. Covalent Adaptable Networks (CANs): A Unique Paradigm in Cross-Linked Polymers. *Macromolecules* **2010**, *43*, 2643−2653.

(10) Zhang, V.; Kang, B.; Accardo, J. V.; Kalow, J. A. Structure − Reactivity − Property Relationships in Covalent Adaptable Networks. *J. Am. Chem. Soc.* **2022**, *144*, 22358−22377.

(11) Wanasinghe, S. V.; Dodo, O.; Konkolewicz, D. Dynamic Bonds: Adaptable Timescales for Responsive Materials. *Angew. Chem., Int. Ed.* **2022**, *61*, No. e202206938.

(12) Chen, X.; Dam, M. A.; Ono, K.; Mal, A.; Shen, H.; Nutt, S. R.; Sheran, K.; Wudl, F. A Thermally Re-Mendable Cross-Linked Polymeric Material. *Science* **2002**, *295*, 1698−1702.

(13) Dello Iacono, S.; Martone, A.; Pastore, A.; Filippone, G.; Acierno, D.; Zarrelli, M.; Giordano, M.; Amendola, E. Thermally Activated Multiple Self-Healing Diels-Alder Epoxy System. *Polym. Eng. Sci.* **2017**, *57*, 674−679.

(14) Shao, C.; Wang, M.; Chang, H.; Xu, F.; Yang, J. A Self-Healing Cellulose Nanocrystal-Poly(Ethylene Glycol) Nanocomposite Hydrogel via Diels-Alder Click Reaction. *ACS Sustainable Chem. Eng.* **2017**, *5*, 6167−6174.

(15) Yang, S.; Du, X.; Deng, S.; Qiu, J.; Du, Z.; Cheng, X.; Wang, H. Recyclable and Self-Healing Polyurethane Composites Based on Diels-Alder Reaction for Efficient Solar-to-Thermal Energy Storage. *Chem. Eng. J.* **2020**, *398*, No. 125654.

(16) Zhou, Q.; Sang, Z.; Rajagopalan, K. K.; Sliozberg, Y.; Gardea, F.; Sukhishvili, S. A. Thermodynamics and Stereochemistry of Diels − Alder Polymer Networks: Role of Crosslinker Flexibility and Crosslinking Density. *Macromolecules* **2021**, *54*, 10510−10519.

(17) Zhang, L.; Rowan, S. J. Effect of Sterics and Degree of Cross-Linking on the Mechanical Properties of Dynamic Poly(Alkylurea − Urethane) Networks. *Macromolecules* **2017**, *50*, 5051−5060.

(18) Chang, J. Y.; Do, S. K.; Han, M. J. A Sol-Gel Reaction of Vinyl Polymers Based on Thermally Reversible Urea Linkages. *Polymer* **2001**, *42*, 7589−7594.

(19) Self, J. L.; Dolinski, N. D.; Zayas, M. S.; Alaniz, J. R.; de Bates, C. M. Brønsted-Acid-Catalyzed Exchange in Polyester Dynamic Covalent Networks. *ACS Macro Lett.* **2018**, *7*, 817−821.

(20) Montarnal, D.; Capelot, M.; Tournilhac, F.; Leibler, L. Silica-Like Malleable Materials from Permanent Organic Networks. *Science* **2011**, *334*, 965−968.

(21) Kamada, J.; Koynov, K.; Corten, C.; Juhari, A.; Yoon, J. A.; Urban, M. W.; Balazs, A. C.; Matyjaszewski, K. Redox Responsive Behavior of Thiol/Disulfide-Functionalized Star Polymers Synthesized via Atom Transfer Radical Polymerization. *Macromolecules* **2010**, *43*, 4133−4139.

(22) Ji, S.; Cao, W.; Yu, Y.; Xu, H. Visible-Light-Induced Self-Healing Diselenide-Containing Polyurethane Elastomer. *Adv. Mater.* **2015**, *27*, 7740−7745.

(23) Fenimore, L. M.; Chen, B.; Torkelson, J. M. Materials Chemistry A. *J. Mater. Chem A* **2022**, *10*, 24726−24745.

(24) Wang, S.; Urban, M. W. Self-Healing Polymers. *Nat. Rev. Mater.* **2020**, *5*, 562−583.

(25) Orrillo, A. G.; Furlan, R. L. E. Sulfur in Dynamic Covalent Chemistry. *Angew. Chem., Int. Ed.* **2022**, *61*, No. e202201168.

(26) Cash, J. J.; Kubo, T.; Dobbins, D. J.; Sumerlin, B. S. Maximizing the Symbiosis of Static and Dynamic Bonds in Self-Healing Boronic Ester Networks. *Polym. Chem.* **2018**, *9*, 2011−2020.

(27) Lessard, J. J.; Garcia, L. F.; Easterling, C. P.; Sims, M. B.; Bentz, K. C.; Arencibia, S.; Savin, D. A.; Sumerlin, B. S. Catalyst-Free Vitrimers from Vinyl Polymers. *Macromolecules* **2019**, *52*, 2105−2111.

(28) Lessard, J. J.; Stewart, K. A.; Sumerlin, B. S. Controlling Dynamics of Associative Networks through Primary Chain Length. *Macromolecules* **2022**, *55*, 10052−10061.

(29) Denissen, W.; De Baere, I.; Van Paepegem, W.; Leibler, L.; Winne, J.; Du Prez, F. E. Vinylogous Urea Vitrimers and Their Application in Fiber Reinforced Composites. *Macromolecules* **2018**, *51*, 2054−2064.

(30) Cai, Y.; Zou, H.; Zhou, S.; Chen, Y.; Liang, M. Room-Temperature Self-Healing Ablative Composites via Dynamic Covalent Bonds for High-Performance Applications. *ACS Appl. Polym. Mater.* **2020**, *2*, 3977−3987.

(31) Lowe, A. B. Thiol-Ene "Click" Reactions and Recent Applications in Polymer and Materials Synthesis. *Polym. Chem.* **2010**, *1*, 17−36.

(32) Zhang, B.; Digby, Z. A.; Flum, J. A.; Chakma, P.; Saul, J. M.; Sparks, J. L.; Konkolewicz, D. Dynamic Thiol-Michael Chemistry for Thermoresponsive Rehealable and Malleable Networks. *Macromolecules* **2016**, *49*, 6871−6878.

(33) Chakma, P.; Rodrigues Possarle, L. H.; Digby, Z. A.; Zhang, B.; Sparks, J. L.; Konkolewicz, D. Dual Stimuli Responsive Self-Healing and Malleable Materials Based on Dynamic Thiol-Michael Chemistry. *Polym. Chem.* **2017**, *8*, 6534−6543.
(34) Ishibashi, J. S. A.; Kalow, J. A. Vitrimeric Silicone Elastomers Enabled by Dynamic Meldrum's Acid-Derived Cross-Links. *ACS Macro Lett.* **2018**, *7*, 482−486.
(35) Zhang, B.; Chakma, P.; Shulman, M. P.; Ke, J.; Digby, Z. A.; Konkolewicz, D. Probing the Mechanism of Thermally Driven Thiol-Michael Dynamic Covalent Chemistry. *Org. Biomol. Chem.* **2018**, *16*, 2725−2734.
(36) Joshi, G.; Anslyn, E. V. Dynamic Thiol Exchange with β-Sulfidor-α,β-Unsaturated Carbonyl Compounds and Dithianes. *Org. Lett.* **2012**, *14*, 4714−4717.
(37) Krenske, E. H.; Petter, R. C.; Houk, K. N. Kinetics and Thermodynamics of Reversible Thiol Additions to Mono- and Diactivated Michael Acceptors: Implications for the Design of Drugs That Bind Covalently to Cysteines. *J. Org. Chem.* **2016**, *81*, 11726−11733.
(38) Serafimova, I. M.; Pufall, M. A.; Krishnan, S.; Duda, K.; Cohen, M. S.; Maglathlin, R. L.; McFarland, J. M.; Miller, R. M.; Frödin, M.; Taunton, J. Reversible Targeting of Noncatalytic Cysteines with Chemically Tuned Electrophiles. *Nat. Chem. Biol.* **2012**, *8*, 471−476.
(39) Zhong, Y.; Xu, Y.; Anslyn, E. V. Studies of Reversible Conjugate Additions. *Eur. J. Org. Chem.* **2013**, *2013*, 5017−5021.
(40) Herbert, K. M.; Getty, P. T.; Dolinski, N. D.; Hertzog, J. E.; de Jong, D.; Lettow, J. H.; Romulus, J.; Onorato, J. W.; Foster, E. M.; Rowan, S. J. Dynamic Reaction-Induced Phase Separation in Tunable, Adaptive Covalent Networks. *Chem. Sci.* **2020**, *11*, 5028−5036.
(41) Herbert, K. M.; Dolinski, N. D.; Boynton, N. R.; Murphy, J. G.; Lindberg, C. A.; Sibener, S. J.; Rowan, S. J. Controlling the Morphology of Dynamic Thia-Michael Networks to Target Pressure-Sensitive and Hot Melt Adhesives. *ACS Appi. Mater. Interfaces* **2021**, *13*, 27471−27480.
(42) Fitzsimons, T. M.; Oentoro, F.; Shanbhag, T. V.; Anslyn, E. V.; Rosales, A. M. Preferential Control of Forward Reaction Kinetics in Hydrogels Crosslinked with Reversible Conjugate Additions. *Macromolecules* **2020**, *53*, 3738−3746.
(43) FitzSimons, T. M.; Anslyn, E. V.; Rosales, A. M. Effect of PH on the Properties of Hydrogels Cross-Linked via Dynamic Thia-Michael Addition Bonds. *ACS Polym. Au* **2022**, *2*, 129−136.
(44) Jackson, G. L.; Dennis, J. M.; Dolinski, N. D.; Van Der Naald, M.; Kim, H.; Eom, C.; Rowan, S. J.; Jaeger, H. M. Designing Stress-Adaptive Dense Suspensions Using Dynamic Covalent Chemistry. *Macromolecules* **2022**, *55*, 6453−6461.
(45) Kuhl, N.; Geitner, R.; Bose, R. K.; Bode, S.; Dietzek, B.; Schmitt, M.; Popp, J.; Garcia, S. J.; van der Zwaag, S.; Schubert, U. S.; Hager, M. D. Self-Healing Polymer Networks Based on Reversible Michael Addition Reactions. *Macromol. Chem. Phys.* **2016**, *217*, 2541−2550.
(46) Sijbesma, R. P.; Beijer, F. H.; Brunsveld, L.; Folmer, B. J. B.; Hirschberg, J. H. K. K.; Lange, R. F. M.; Lowe, J. K. L.; Meijer, E. W. Reversible Polymers Formed from Self-Complementary Monomers Using Quadruple Hydrogen Bonding. *Science* **1997**, *278*, 1601−1604.
(47) Manjunatha, B.; Bodke, Y. D.; Jain, S. K.; Lohith, L. N.; Sridhar, M. A. Novel Isoxazolone Based Azo Dyes: Synthesis, Characterization, Computational, Solvatochromic UV-Vis Absorption and Biological Studies. *J. Mol. Struct.* **2021**, *1244*, No. 130933.
(48) Jurberg, I. D. An Aminocatalyzed Stereoselective Strategy for the Formal α-Propargylation of Ketones. *Chem.−Eur. J.* **2017**, *23*, 9716−9720.
(49) Hammett, L. P. The Effect of Structure upon the Reactions of Organic Compounds. Temperature and Solvent Influences. *J. Chem. Phys.* **1936**, *4*, 613−617.
(50) Zhang, X.; Wang, J.-H.; Tan, D.; Li, Q.; Li, M.; Gong, Z.; Tang, C.; Liu, Z.; Dong, M.; Lei, X. Carboxylate-Selective Chemical Cross-Linkers for Mass Spectrometric Analysis of Protein Structures. *Anal. Chem.* **2018**, *90*, 1195−1201.
(51) Lei, X.; Jones, A.; Dong, M.; Cao, Y.; Tan, H. Chemical Crosslinking Agent for Protein and Preparation Method and Application Thereof. CN107628937A2018.
(52) Jha, N.; Singh, R. P.; Saxena, P.; Kapur, M. Iridium(III)-Catalyzed C(3)-H Alkylation of Isoquinolines via Metal Carbene Migratory Insertion. *Org. Lett.* **2021**, *23*, 8694−8698.
(53) Fortman, D. J.; Brutman, J. P.; Hillmyer, M. A.; Dichtel, W. R. Structural Effects on the Reprocessability and Stress Relaxation of Crosslinked Polyhydroxyurethanes. *J. Appl. Polym. Sci.* **2017**, *134*, 44984.
(54) Bin Rusayyis, M. A.; Torkelson, J. M. Reprocessable Covalent Adaptable Networks with Excellent Elevated-Temperature Creep Resistance: Facilitation by Dynamic, Dissociative Bis(Hindered Amino) Disulfide Bonds. *Polym. Chem.* **2021**, *12*, 2760−2771.
(55) Hirao, T.; Hisano, N.; Akine, S.; Kihara, S. I.; Haino, T. Ring-Chain Competition in Supramolecular Polymerization Directed by Molecular Recognition of the Bisporphyrin Cleft. *Macromolecules* **2019**, *52*, 6160−6168.

https://doi.org/10.1021/jacs.3c03643
J. Am. Chem. Soc. XXXX, XXX, XXX−XXX